

Structural Differentiation of the *Bacillus subtilis* 168 Cell Wall

L. L. GRAHAM* AND T. J. BEVERIDGE

Department of Microbiology, College of Biological Sciences, University of Guelph,
Guelph, Ontario, Canada N1G 2W1

Received 23 August 1993/Accepted 19 November 1993

Exponential-growth-phase cultures of *Bacillus subtilis* 168 were probed with polycationized ferritin (PCF) or concanavalin A (localized by the addition of horseradish peroxidase conjugated to colloidal gold) to distinguish surface anionic sites and teichoic acid polymers, respectively. Isolated cell walls, lysozyme-digested cell walls, and cell walls treated with mild alkali to remove teichoic acid were also treated with PCF. After labelling, whole cells and walls were processed for electron microscopy by freeze-substitution. Thin sections of untreated cells showed a triphasic, fibrous wall extending more than 30 nm beyond the cytoplasmic membrane. Measurements of wall thickness indicated that the wall was thicker at locations adjacent to septa and at pole-cylinder junctions ($P < 0.001$). Labelling studies showed that at saturating concentrations the PCF probe labelled the outermost limit of the cell wall, completely surrounding individual cells. However, at limiting PCF concentrations, labelling was observed at only discrete cell surface locations adjacent to or overlying septa and at the junction between pole and cylinder. Labelling was rarely observed along the cell cylinder or directly over the poles. Cells did not label along the cylindrical wall until there was visible evidence of a developing septum. Identical labelling patterns were observed by using concanavalin A-horseradish peroxidase-colloidal gold. Neither probe appeared to penetrate between the fibers of the wall. We suggest that the fibrous appearance of the wall seen in freeze-substituted cells reflects turnover of the wall matrix, that the specificity of labelling to discrete sites on the cell surface is indicative of regions of extreme hydrolytic activity in which α -glucose residues of the wall teichoic acids and electronegative sites (contributed by phosphate and carboxyl groups of the teichoic acids and carboxyl groups of the peptidoglycan polymers) are more readily accessible to our probes, and that the wall of exponentially growing *B. subtilis* cells contains regions of structural differentiation.

The cell wall of *Bacillus subtilis* 168 is a two-polymer structure comprised virtually of teichoic acids (54%) and peptidoglycan (46%) on a per dry weight basis when cultured in Spizizen minimal medium (4, 30, 31). Despite this chemical simplicity, the exact mechanisms by which the wall grows, divides, and turns over have not been adequately explained (2).

Numerous studies indicate that the predominant mode of wall growth involves insertion of newly synthesized wall polymers in an inside-to-outside fashion at many sites randomly distributed along the cytoplasmic membrane (21, 22). According to the surface stress theory of Koch (18), this newly inserted material is cross-linked to the existing wall fabric at the inner wall surface but is unstressed. It assumes tension only after it is pushed outwards by more recently acquired wall material. Select bonds in this "stretched" wall eventually undergo hydrolysis, turning over or releasing polymers from the cell surface. It is the addition of new polymers at many sites along the membrane to the inner wall surface and the stretching of these polymers as they are displaced towards the wall's outermost periphery which allows the cell to elongate.

Polycationic ferritin (PCF) has been used successfully as a probe for localization of anionic sites on the surfaces of gram-positive cells such as *B. subtilis* (10) and *Streptococcus faecalis* (32). Sonnenfeld et al. (28) reported that dilute solutions of PCF had great affinity for cell surface sites expressing high electronegativity and showed that isolated cell walls of *B. subtilis* could be partially differentiated by surface charge. Chemical modification of isolated walls indicated that the anionic nature of *B. subtilis* cell walls was due primarily to

the carboxyl groups of muramyl peptides and phosphate groups of teichoic acids (29).

The lectin concanavalin A (ConA) has been used to localize α -D-glucose residues in walls containing teichoic acid polymers (5). Beveridge and Murray (3) used ConA conjugated to ferritin to outline the inner and outer limits of walls isolated from the 168 strain during their metal-binding study and proved that teichoic acid was exposed on both sides of the wall. Using radiolabelled ConA, Lang and Archibald (19) showed that a linear relationship existed between ConA binding and surface-exposed teichoic acids and that there was no cooperativity of binding (i.e., the system exhibited first-order kinetics).

In concert, all of these studies suggest that the surface of *B. subtilis* has an overall electronegative charge at neutral pH, that the charge is due to exposed carboxyl and phosphate groups which emanate from the peptidoglycan and teichoic acid polymers, respectively, and that select regions of the surface possess a greater net charge than those of others. These results have been obtained through kinetic analyses either of bulk suspensions of the bacterium or of cells conventionally processed for electron microscopy (EM). Our freeze-substitution regimen, which preserves cellular constituents, especially cell wall polymers, better than conventional means, has shown that the cell wall of *B. subtilis* 168 possesses much more infrastructure in thin-section profile than originally suspected (13, 14). In light of these new observations, it was important to reexamine charge distribution and teichoic acid location using this new cryotechnique. This report correlates previous observations of wall charge differentiation with wall infrastructure, redefines sites of surface structural differentiation, and relates these results to wall turnover, cell elongation, and cell division in *B. subtilis*.

(A portion of this data has been presented previously [14a].)

* Corresponding author. Present address: Department of Biology, St. Francis Xavier University, Antigonish, Nova Scotia, Canada B2G 2W5. Phone: (902) 867-2386. Fax: (902) 867-5153.

MATERIALS AND METHODS

Culture conditions. *B. subtilis* 168 cells were maintained on slants of brain heart infusion agar (Difco). For culture, a 1% inoculum of an exponential-growth-phase culture grown in Spizizen minimal medium (30) supplemented with 50 µg of L-tryptophan (Sigma Chemical Co.) per ml, 2 mg of casein hydrolysate (Difco) per ml, and 0.5% (vol/vol) glycerol (Fisher Scientific Co.) was inoculated into fresh supplemented Spizizen medium and grown at 37°C and 150 rpm for 5 h to mid-exponential phase (optical density at 600 nm [OD₆₀₀] = 0.675). Cells were harvested by centrifugation (10 min, 8,000 × g), washed once to remove contaminating medium components, and resuspended to an OD₆₀₀ of 0.8 either in 0.05 M *N,N*-2-hydroxyethylpiperazine-*N'*-2-ethanesulfonic acid (HEPES; Research Organics Inc.) buffer (pH 6.8) for PCF treatment or in 0.05 M Tris (pH 7.0) containing 0.15 M NaCl for ConA treatment.

Isolation of cell walls. Cell walls were obtained from exponentially growing cultures of *B. subtilis* as described previously (3). The purity of the wall fragments was ascertained by EM (negative stains and thin sections) and by testing for NADH oxidase as a marker for plasma membrane enzymes (23). Some wall fragments were partially digested with lysozyme (Sigma; 10 µg/ml in 0.05 M HEPES buffer [pH 7.3]) for 1 h at 37°C. Isolated walls were also treated with 0.1 N NaOH under nitrogen gas at 35°C for 24 h (17) to extract teichoic acids. The efficiency of the extraction was determined by estimates of phosphorus (9).

PCF labelling. PCF (11.0 mg of ferritin per ml of *N,N*-dimethyl-1,3-propanediamine [Sigma]) was diluted 1:1 with 0.05 M HEPES buffer (pH 6.8), dialyzed against buffer for 6 h at 4°C to remove salts, and stored as 100-µl aliquots at -20°C until used. Prior to use it was centrifuged (30 s, 14,000 × g; Eppendorf) to remove aggregates. To determine saturating versus limiting concentrations of PCF as a surface probe, a range of concentrations was used; PCF was diluted in HEPES buffer at 1:50, 1:100 (saturating concentration), 1:150, 1:200, and 1:500 to obtain final concentrations of 55, 27.5, 20.6, 13.75, and 5.5 µg/ml, respectively, in the bacterium-PCF reaction mixture. These final reaction mixtures, consisting of 500 µl of *B. subtilis* cells and 500 µl of PCF, were incubated for 15 min at 22°C on a rotary platform. Cells and bound PCF were pelleted by centrifugation (45 s, 14,000 × g; Eppendorf), washed five times in 1.5-ml aliquots of fresh buffer, and processed for EM.

Isolated cell walls, lysozyme-digested walls, and alkali-treated walls were suspended at 1 mg/ml in HEPES buffer. Labelling was performed for 15 min using PCF diluted 1:50 (55 µg/ml) in a final reaction mixture consisting of 100 µl of PCF and 100 µl of cell walls. Walls were washed as described above and processed for EM.

ConA labelling. ConA (Inter Medico) was reconstituted at 2 mg/ml (stock solution, 0.2% [wt/vol]) in 0.05 M Tris buffer (pH 7.0) containing 0.15 M NaCl (as recommended by manufacturer), aliquoted into 100-µl volumes, and stored at -20°C until necessary. For labelling, 100 µl of this stock solution was used undiluted or diluted in buffer (1:5 or 1:10) and mixed with 900 µl of bacteria (OD₆₀₀ = 0.8) to obtain final ConA concentrations of 200 µg/ml (0.02%), 40 µg/ml (0.004%), and 20 µg/ml (0.002%) in the bacterium-ConA reaction mixture. Cells and ConA were incubated for 30 min at 22°C on a rotary platform, washed twice with fresh buffer to remove unbound ConA, and resuspended in 1 ml of buffer. The location of ConA was determined by the addition of 75 ng (20 µl of a 3.75-µg/ml solution) of horseradish peroxidase conju-

gated to colloidal gold (HRP-gold; Inter Medico). Cells were incubated for an additional 30 min at 22°C, washed three times in buffer to remove unbound HRP-gold, and processed for EM.

To ensure the specificity of ConA labelling, α-methyl mannoside (Sigma) was used as a competitive inhibitor. ConA (100 µl of 2-mg/ml stock) was incubated for 15 min at 22°C in the presence of 100 µl of buffer or 100 µl of 160 µM α-methyl mannoside, at which time 800 µl of *B. subtilis* cells (OD₆₀₀ = 0.7) was added, and the mixture incubated for an additional 30 min at 22°C on a rotary platform. Cells were washed twice with buffer to remove unbound ConA, and 20 µl of HRP-gold was added. After 30 min, cells were washed and examined directly by EM as unstained whole mounts to check for the presence of colloidal gold label.

Freeze-substitution. Freeze-substitution was performed as previously described (13, 14). Untreated cells, cells treated with PCF or ConA-HRP-gold, and PCF-treated cell walls were mixed with an equal volume of molten 2% (wt/vol) Noble agar (ca. 60°C), and each was immediately layered onto a cellulose-ester membrane (Gelman Sciences). Wedge-shaped portions of each filter were plunge-frozen in liquid propane as a cryogen (-189°C) and immediately transferred onto frozen (-196°C) substitution medium. Substitution medium consisted of 2% (wt/vol) osmium tetroxide and 2% (wt/vol) uranyl acetate in anhydrous acetone (all reagents from Fisher) in the presence of a molecular sieve (sodium aluminosilicate; pore diameter, 0.4 nm; Sigma). Samples were substituted for 72 h at -80°C, after which time the vials were warmed to room temperature and excess fixative was removed by six changes in fresh anhydrous acetone (each for a 15-min duration). Samples were infiltrated overnight at room temperature in an acetone-Epon 812 mixture (1:1), embedded in fresh Epon 812, and polymerized at 60°C for 36 h.

EM. All samples were thin sectioned on a Reichert-Jung Ultracut E ultramicrotome and mounted on Formvar carbon-coated copper grids. When necessary, sections were stained with 2% (wt/vol) aqueous uranyl acetate and lead citrate (26). EM was performed with a Philips EM300 electron microscope at an operating voltage of 60 kV under standard operating conditions with the cold trap in place.

Statistical analyses. Measurements of wall width were made on images enlarged 10 times from negatives obtained by EM (final magnification, ×111,020). The wall width was measured at four separate locations on the cell wall of each cell as indicated Fig. 1A. The wall was defined as all the material between the outer face of the plasma membrane and the outermost region of the fibrous wall. Measurements were not made directly over septal regions as it was difficult to determine the exact orientation, position, and maturity of the septum compared with the other cell wall regions. Only cells cross-sectioned longitudinally to reveal complete envelope profiles, including the plasma membrane bilayer, were considered. Transverse sections of walls and sections of cells positioned too close together to enable distinction between individual cell walls were disregarded. A one-way analysis of variance and the Tukey test for multiple comparisons (33) were used to determine the significance of wall width measurements at the selected sites.

Cells treated with ConA-HRP-gold were enumerated for the presence of gold label. Data were evaluated by using a chi-square test (33) to determine differences in the frequency of labelling at the same four locations on the cell wall.

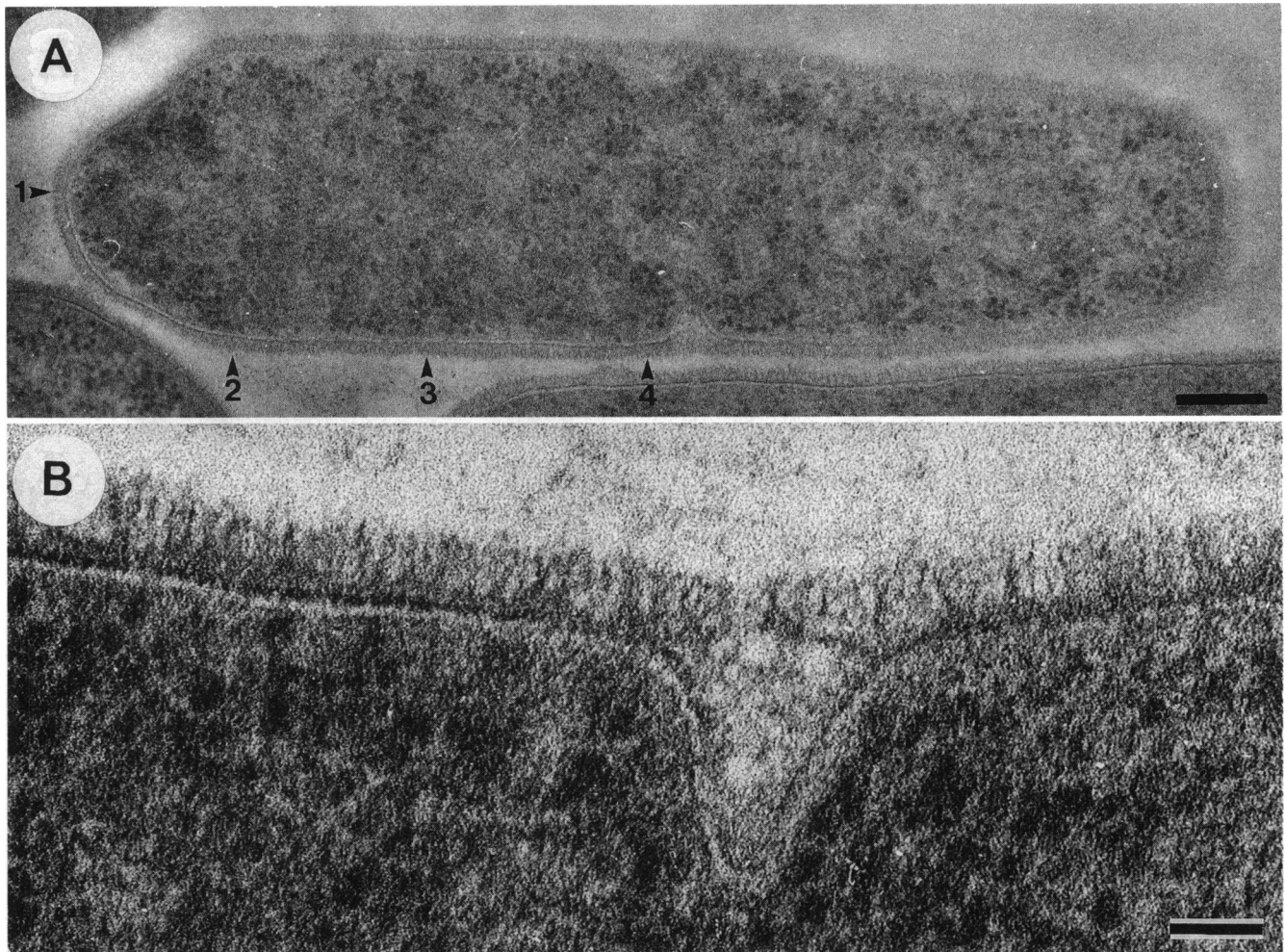


FIG. 1. (A) Freeze-substituted image of an exponentially growing *B. subtilis* 168 cell showing the fibrous cell wall. Arrows indicate the four locations at which wall thickness measurements were taken. Numbers correspond to the sites listed in Table 1. Bar, 200 nm. (B) High-magnification image of the cell wall showing its triphasic nature. Note the infrastructure visible at the developing septum. Bar, 50 nm.

RESULTS

Wall structure and thickness. Thin-section envelope profiles of freeze-substituted *B. subtilis* cells revealed a fibrous cell wall 30 to 40 nm in thickness extending perpendicularly away from the plasma membrane (Fig. 1A). The wall was tripartite (Fig. 1B), with the innermost layer, that immediately adjacent to the outer leaflet of the plasma membrane, being most electron dense. The intermediate layer, 10 to 15 nm in thickness, and the outermost fibrous layer, which extended an additional 15 to 20 nm, were each of lower electron density. Measurements of total wall thickness revealed that the wall at pole and cylinder regions was 30 to 35 nm in thickness whereas that at cylinder-septum and pole-cylinder junctions was consistently thicker, 38 to 40 nm in thickness ($P \leq 0.001$) (Table 1).

PCF labelling. At saturating concentrations (55 and 27.5 $\mu\text{g/ml}$), PCF completely surrounded individual cells, localizing at the periphery of the wall fabric in a tightly packed formation (Fig. 2). Decreasing the concentration of PCF (i.e., 5.5 or 13.75 $\mu\text{g/ml}$) abolished this close packing and resulted in more PCF label at select surface sites, adjacent to and over septal regions and at pole-cylinder junctions (Fig. 3). Labelling at these sites was retained throughout the cell division cycle. Although PCF particles labelled the wall surface adjacent to and overlying

septa, the probe did not penetrate the septum until the two daughter cells were nearly separated. PCF did not penetrate the wall fabric to the electron-dense inner layers and did not align along the length of individual wall fibers. At dilute PCF concentrations (less than 5.5 $\mu\text{g/ml}$), minimal PCF labelling was observed over the poles or along the length of the cell cylinder in the absence of septa.

PCF labelling of isolated walls. Freeze-substituted cell walls isolated from *B. subtilis* revealed the same fibrous appearance as whole cells with PCF labelling restricted to the outer surface of the walls only (Fig. 4). Unstained whole mounts revealed the

TABLE 1. Cell wall thickness at four sites on *B. subtilis* 168 cells

Site no. ^a	Site	Wall thickness ^b (\pm SD) (nm)
1	Pole	34 (2)
2	Pole-cylinder	38 (6)
3	Cylinder	34 (5)
4	Cylinder-septum	41 (5)

^a The site number corresponds to the numbering in Fig. 1A.

^b Each thickness is the mean of measurements made on 30 different cells.

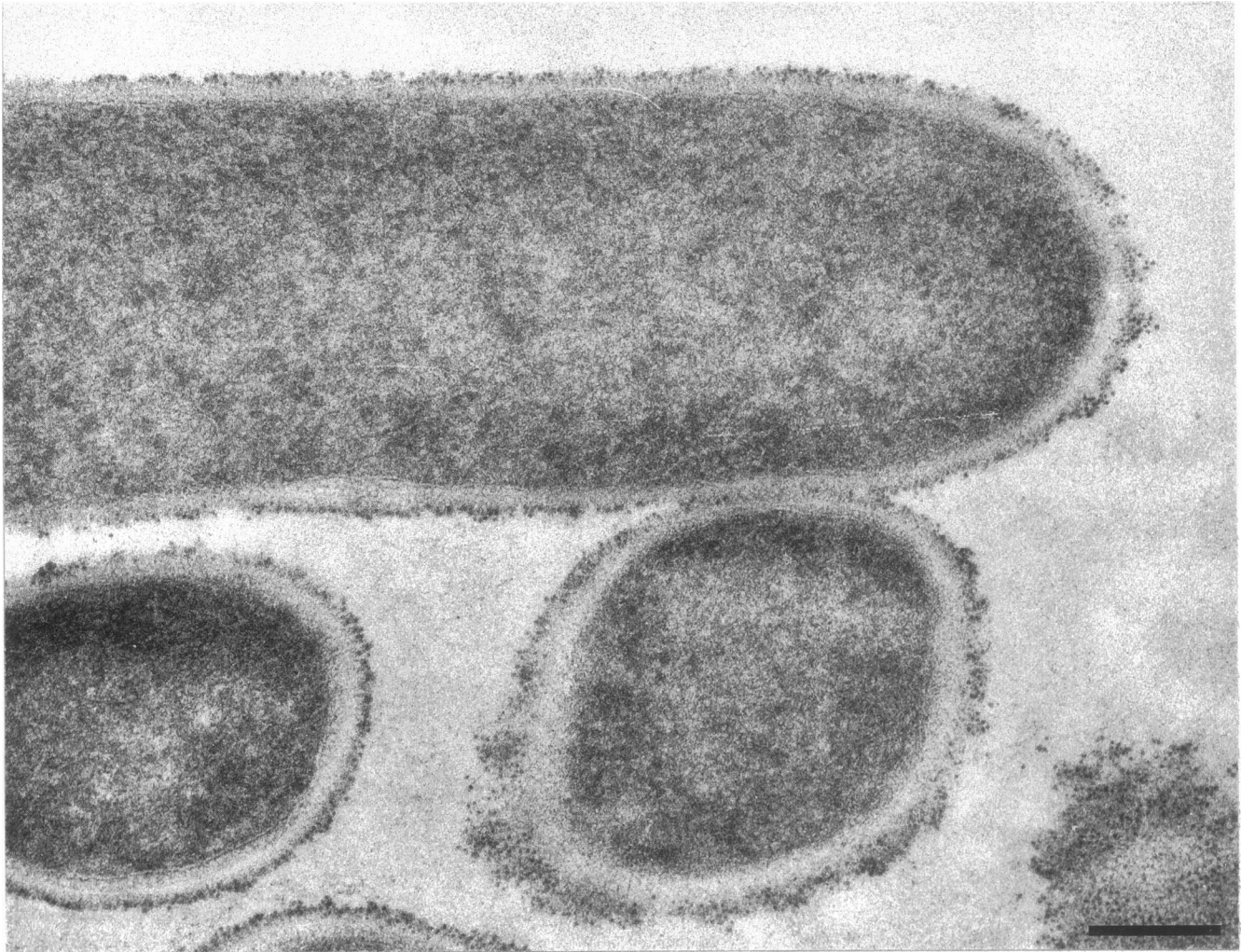


FIG. 2. Labelling of the outer surface of the cell wall with saturating concentrations of PCF. Note that the cells are completely surrounded by the probe and that the PCF does not penetrate into the wall matrix. Bar, 200 nm.

probe to be randomly scattered across the wall (data not shown). Cell wall fragments treated with lysozyme or alkali revealed the PCF-binding asymmetry to be lost and also displayed severely disrupted ultrastructure in which much of the fibrous matrix was lost or disorganized. Whole mounts revealed less PCF binding, a finding also reflected in thin section (data not shown). Determination of site-specific labelling was not possible since isolated walls tended to collapse during processing, losing their rod shape, and since higher concentrations of PCF were used to ensure labelling of treated walls.

ConA labelling. Cells treated with low concentrations of ConA (20 to 40 $\mu\text{g/ml}$) also revealed the specific distribution of label over septal sites and at pole-cylinder junctions ($P < 0.001$). Minimal labelling was apparent over the poles or along the length of the cell cylinder (Fig. 5). Labelling with ConA was completely abolished when assayed in the presence of α -methyl mannoside, indicating specificity of this probe for the α -glucose residues of the teichoic acid polymers (data not shown).

As with PCF, ConA was located only at the extreme outer edge of the fibrous cell wall. This probe did not penetrate to the more electron dense inner regions of the wall fabric nor did

it align along the length of individual fibers. Rather, it remained localized at the outermost edge of the wall fabric, and only in the late stages of cell separation was penetration between daughter cells observed. The labelling of isolated cell walls was also consistent with that seen with the PCF experiments.

DISCUSSION

Thin-section EM images of conventionally prepared *B. subtilis* cells show, overlying the plasma membrane, a wall of electron-dense amorphous material that is approximately 25 nm in thickness (13) devoid of any infrastructure. Freeze-etch data reveal that the *B. subtilis* cell wall lacks internal fracture planes, implying that the entire wall fabric must be of one structural form in which covalent bonds predominate (1).

Unfortunately, these data do not correlate with the dynamic qualities required for a structural system such as this. The gram-positive wall is a stress-bearing structure designed to resist the cell's turgor pressure and requires constant maintenance (to discourage spheroplasting) and remodeling (to incorporate new wall material and ensure cellular growth and division). In Koch's inside-to-outside model of wall growth

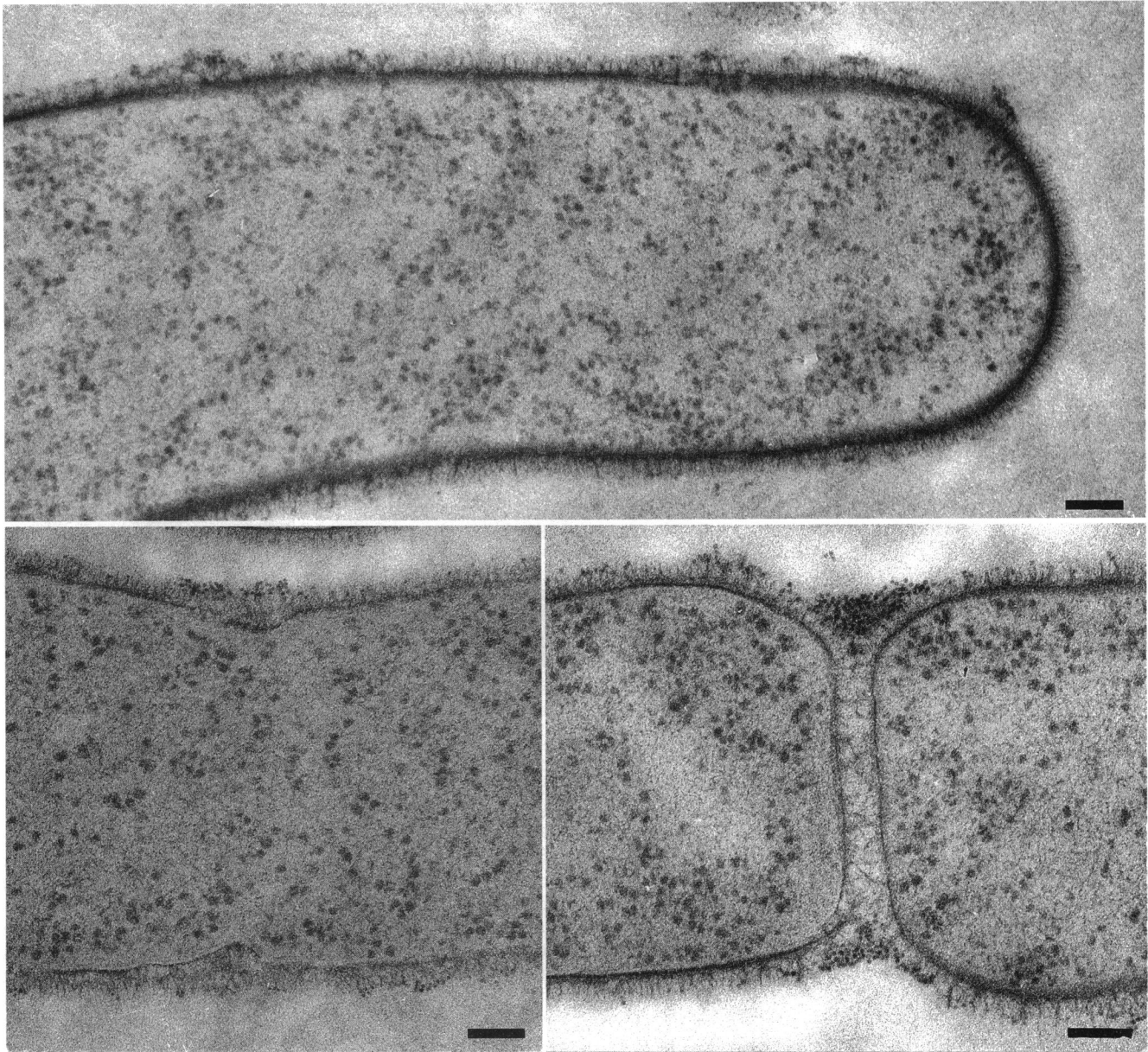


FIG. 3. Labelling of whole cells with minimal concentrations of PCF. Note the presence of PCF at pole-cylinder junctions and over septal sites. Bars, 100 nm.

(18) the integrity of the wall fabric is never disrupted during cell growth because new polymers enter and are covalently incorporated into the existing wall matrix before older bonds, situated further from the membrane, are stretched and eventually hydrolyzed to release wall material from the cell surface (8). "Aging" of the wall fabric as it progresses from the inner cytoplasmic surface to the outermost edge where it is turned over is well documented (6, 21, 24, 25).

Autoradiography and fluorescence microscopy indicate that insertion of new wall polymers occurs uniformly along the cell cylinder whereas insertion, and hence turnover, occurs much more slowly over the pole regions (22). In fact, polar wall may be six generations older than cylindrical wall (6). But wall material may be added to the poles via two distinct processes, an inside-to-outside growth similar to that observed along the

cylinder (although at a reduced rate) as well as by lateral spreading of wall polymers into the pole region from the adjacent cylindrical wall. The combination of slow turnover and spreading of polymers into the pole region requires that this junction be composed of wall quite different from that which composes the cylinder. Unlike the remainder of the wall, septa constitute mostly newly synthesized material (22), as would be expected for a region destined to become a new polar cap.

While these studies provide insight into the process of wall turnover, they have not described the polymeric organization of the wall. Early EM studies by Birdsell et al. (5) suggested that teichoic acid polymers were oriented perpendicular to the long axis of the cell. Sonnenfeld et al. (28) concluded from conventional embedding and thin sectioning of isolated *B.*

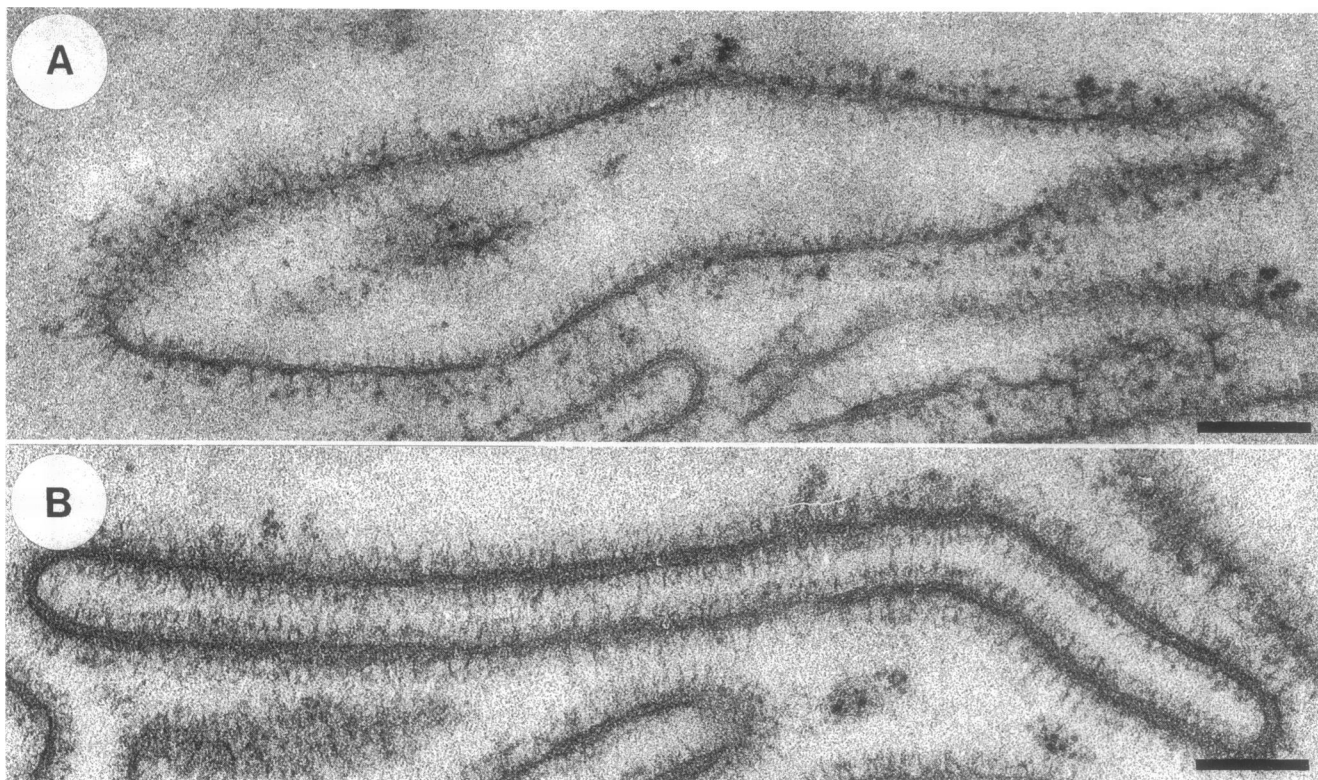


FIG. 4. Isolated *B. subtilis* walls labelled with PCF and processed by freeze-substitution. (A) No postsection staining; (B) stained with uranyl acetate and lead citrate. Note the presence of the probe on the external wall surface only. Bars, 100 nm.

subtilis cell walls labelled with low concentrations of PCF that the asymmetry of label distribution at pH 7 (labelling was localized at the outer wall face at the pole-cylinder junction; no labelling was observed over septa or on the inner face of the wall) was due to the orientation of free electronegative charges possessed by teichoic acids and muramyl peptides positioned towards the outside of cell wall, each charge group existing above the plane of the glycan strands in an orientation which would allow maximum accessibility of the probe to exposed anionic sites within the wall.

Freeze-substitution has recently been shown to be superior to conventional preparatory methods for the accurate preservation of bacterial cell ultrastructure (13) and for the retention of fragile structures such as fibrous cell walls (12, 15). By labelling native cells with specific wall polymer probes prior to freeze-substitution and EM, we feel that we have come as close as currently possible to authentically localizing specific chemical sites on the *B. subtilis* 168 cell surface. These sites express the strongest electronegativity in the wall and are richest in teichoic acids; they, in turn, represent sites of greatest autolytic activity and wall turnover since cleavage of wall polymers must increase the availability of reactive groups.

Freeze-substitution of rapidly growing *B. subtilis* 168 cells revealed a structurally complex gram-positive cell wall in which wall fibers, arranged perpendicularly to the plasma membrane, extended 30 to 40 nm from the cell surface (13, 14). The triphasic appearance of this wall may be a structural representation of wall growth and turnover in which the electron dense innermost layer, adjacent to the membrane, represents the region of incorporation of newly synthesized wall polymers. It was not possible to discern the outer leaflet of the plasma membrane. Since the lipid moiety of lipoteichoic acid resides

in the plasma membrane, these polymers may be partially responsible for the close adhesion of the wall to the membrane's outer face. Also, it is likely that the associated increase in thickness (measurements indicate that this layer is too thick to represent only the outer leaflet of the plasma membrane) represents the membrane plus new wall material. The enhanced electron density of this inner wall is due to the compacted nature of the wall polymers (these wall polymers are not fully cross-linked; new material is constantly moving in). The presence of free teichoic and lipoteichoic acids in addition to peptidoglycan all contribute electronegative charge groups which bind UO^{2+} ions and stain very darkly (Fig. 6). As defined by Koch's inside-to-outside growth model (18), the middle wall region of intermediate electron density is comprised of intact, fully cross-linked polymers. Within this stress-bearing region, wall polymers are stretched. The wall fabric peripheral to this middle region has already come under autolytic attack, breaking bonds and initiating release of polymers from the matrix. Release of this material is observed structurally in images of freeze-substituted cells as a decrease in electron density and a fibrous appearance. Indeed, the distinct differences in wall thickness at the cylinder-pole junctions and adjacent to septal sites versus the side walls and poles may actually reflect differences in the degree of hydrolysis at these two regions. This would also be substantiated by the degree of PCF or ConA-HRP-gold binding since new carboxyl groups (contributed by peptidoglycan polymers) and phosphate groups and glucose residues (teichoic acids) would be continually and more rapidly exposed at the outer wall face of these two sites. Under saturating conditions, enough PCF or ConA is present to label all exposed chemical sites, resulting in particle saturation of the cell surface (Fig. 2). Yet under

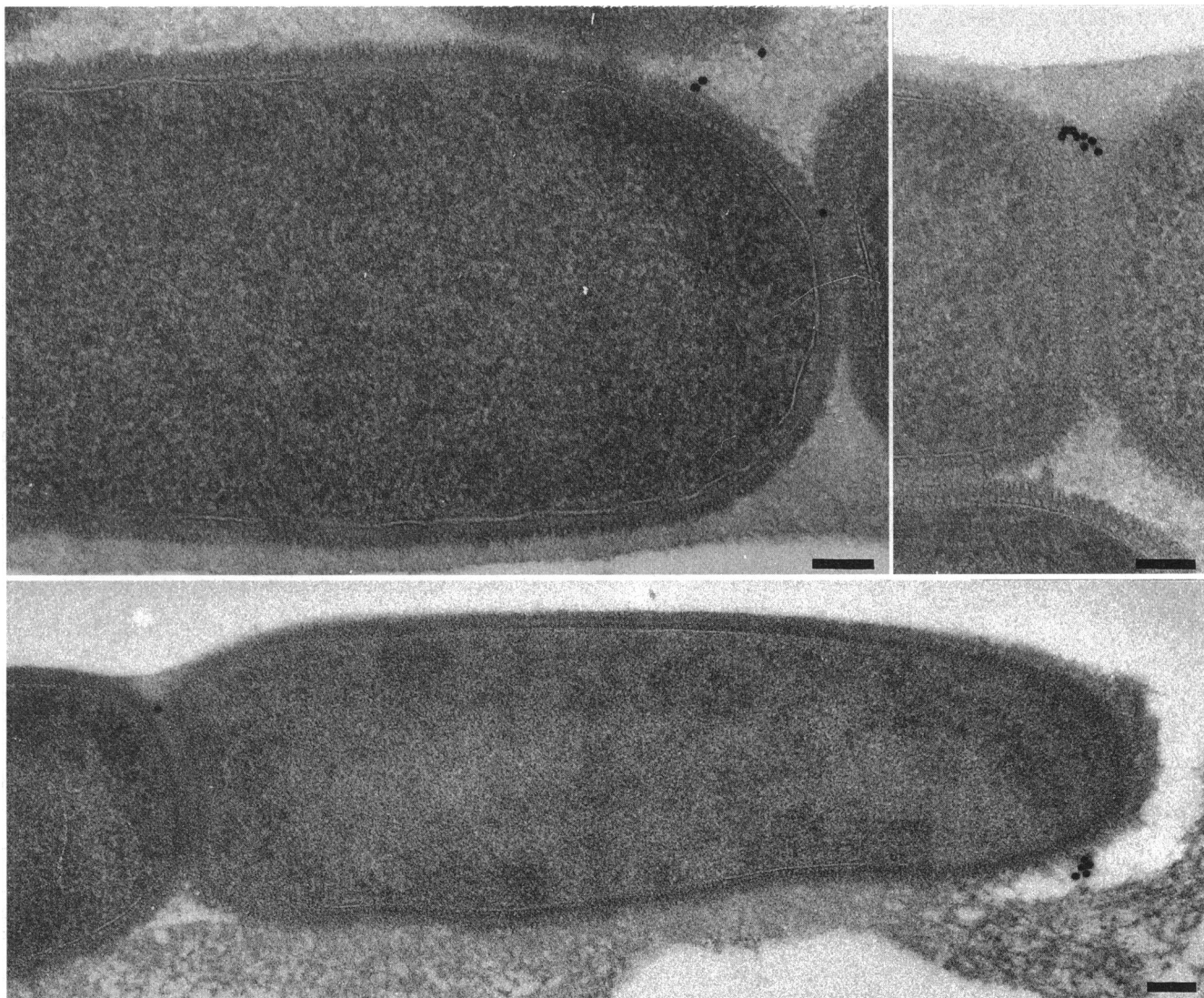


FIG. 5. Labelling of whole cells with ConA-HRP-gold. Note the absence of label over cell poles and along the cell cylinder. Bars, 100 nm.

limiting conditions only those sites with an extreme anionic character (PCF) or with an abundance of teichoic acid (ConA) would label consistently well. Poles (low turnover) and cylindrical wall (steady-state turnover) would not label as well as septal sites and pole-cylinder junctions, regions of greater hydrolytic activity. Labelled sites are the most active regions of wall growth and reflect the tremendous incorporation of wall polymers at cell septa and the remodeling of preexisting polymers at cylinder-pole junctions.

Doyle et al. (7) state that the wall-pole junction undergoes very rapid turnover although Clarke-Sturman et al. (6) suggest that it is a region resistant to turnover, with resistance reflecting a structural difference in the wall at this location. The pole-cylinder junction is the site of contact between new wall polymers from the cylinder and older wall polymers from the pole. Incorporation of wall material of different ages into a stable structure requires rearrangement of peptidoglycan cross-linking such that existing linkages be broken and new ones be formed to create links between old pole polymers and newer cylinder polymers (6). Bond rearrangement coupled with increased stretching of outermost wall polymers (as

polymers are rearranged to fit the curve entering the pole) may have resulted in an increase in the number of available binding sites for the probes utilized in our study.

Incorporation of newly synthesized wall material occurs at evenly distributed locations along the length of the cell cylinder and to a lesser extent over the poles (21, 22); teichoic acids are inserted simultaneously with new peptidoglycan polymers (20). Electronegative sites and glucose residues must, therefore, be present across the entire cell wall. Our study has used intact cells, and our probes are too large (i.e., PCF, 11-nm diameter; colloidal gold, 15-nm diameter) to penetrate deeply into the wall without prior disruption of its fabric. Only at the latest stages of cell division were the probes observed within the fibrous septal sites. Penetration of the probes at this time is likely due to an increase in wall porosity as polymers are attacked by autolysins to enable separation of daughter cells. Indeed, Hobot and Rogers (16) were able to localize *N*-acetylmuramyl-L-alanine amidase to the septal sites of *B. subtilis* 168 cells, using immuno-EM. In our study, untreated isolated walls retained an asymmetry of charge since they bound PCF only on the external surface but required disrup-

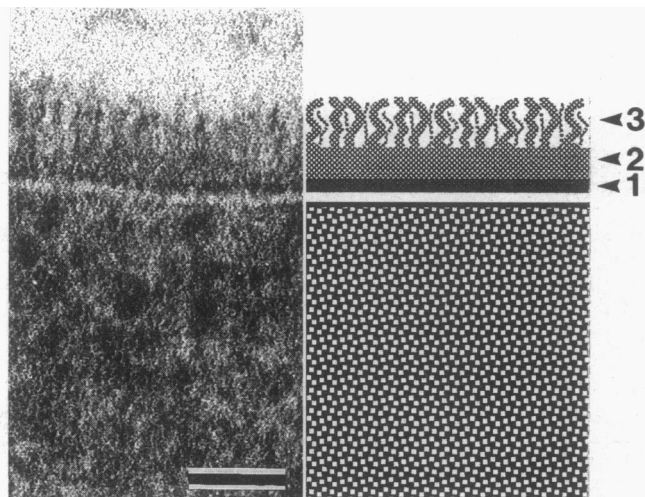


FIG. 6. High-magnification image of a freeze-substituted *B. subtilis* cell wall and corresponding schematic representation. Arrows and numbers indicate the three layers of the wall: 1, innermost layer, outer leaflet of the plasma membrane and newly synthesized wall polymers; 2, intermediate stress-bearing layer; 3, peripheral fibrous layer. Bar, 50 nm.

tion with lysozyme or alkali before PCF penetrated into the wall matrix, confirming previous findings (28, 29).

The perception of the gram-positive cell wall as an amorphous rigid layer is being modified to one of a dynamic, more flexible structure essential for the maintenance of cell shape and turgor pressure, yet able to accommodate growth and elongation. That it is a meshwork of peptidoglycan and secondary polymers is apparent in our images of freeze-substituted cells. Even though Scherrer and Gerhardt (27) have suggested that the peptidoglycan-teichoic acid fiber radius is 0.5 to 1.0 nm and that the fibers exist as single strands rather than bundles, it is unlikely that the fibers which we are seeing at the surface of freeze-substituted cell walls are individual wall fibers because of the superimposition of wall matrix components in thin section (ca. 65 nm thick). Close to the cell membrane (i.e., the inner wall), it is likely that wall polymers are aligned parallel or slightly askew to the plasma membrane (1) although their exact orientation in the wall matrix has not yet been determined. Permeability studies of the cell walls of *Bacillus megaterium* have indicated a biphasic wall composed of an outer wall able to exclude particles that are 2 nm in diameter and a coarse inner wall with pores exceeding 27 nm in diameter (11). These studies are difficult to correlate with our present EM studies and the inside-to-outside growth model (18), which describes three separate regions in the wall: an outermost loose and fibrous region, a taut stress-bearing middle region, and a compacted newly synthesized innermost region. It is possible that the outermost region is so loosely knit and its porosity is so great that Gerhardt and Scherrer (11) did not detect it with their porosity experiments. Alternatively, since they used isolated cell walls, the outermost wall layer may have been removed or damaged during isolation procedures. If either were the case, then their outer layer would correspond to our middle stress-bearing region and their inner layer would correspond to the newly synthesized innermost region.

ACKNOWLEDGMENTS

This research was supported by a Medical Research Council of Canada operating grant to T.J.B. All microscopy was performed in the

NSERC Guelph Regional STEM Facility, which is maintained by funds from the Department of Microbiology and the Natural Sciences and Engineering Research Council of Canada.

REFERENCES

1. Beveridge, T. J. 1981. Ultrastructure, chemistry, and function of the bacterial wall. *Int. Rev. Cytol.* **72**:229-317.
2. Beveridge, T. J. 1988. The bacterial surface: general considerations towards design and function. *Can. J. Microbiol.* **34**:363-372.
3. Beveridge, T. J., and R. G. E. Murray. 1976. Uptake and retention of metals by cell walls of *Bacillus subtilis*. *J. Bacteriol.* **127**:1502-1518.
4. Beveridge, T. J., and R. G. E. Murray. 1980. Sites of metal deposition in the cell wall of *Bacillus subtilis*. *J. Bacteriol.* **141**:876-887.
5. Birdsell, D. C., R. J. Doyle, and M. Morgenstern. 1975. Organization of teichoic acid in the cell wall of *Bacillus subtilis*. *J. Bacteriol.* **121**:726-734.
6. Clarke-Sturman, A. J., A. R. Archibald, I. C. Hancock, C. R. Harwood, T. Merad, and J. A. Hobot. 1989. Cell wall assembly in *Bacillus subtilis*: partial conservation of polar wall material and the effect of growth conditions on the pattern of incorporation of new material at the polar caps. *J. Gen. Microbiol.* **135**:657-665.
7. Doyle, R. J., J. Chaloupka, and V. Vinter. 1988. Turnover of cell walls in microorganisms. *Microbiol. Rev.* **52**:554-567.
8. Doyle, R. J., and A. L. Koch. 1987. The functions of autolysins in the growth and division of *Bacillus subtilis*. *Crit. Rev. Microbiol.* **15**:169-222.
9. Dryer, R. L., A. R. Tammes, and J. I. Routh. 1957. The determination of phosphorus and phosphatase with *N*-phenyl-*p*-phenylenediamine. *J. Biol. Chem.* **225**:117-183.
10. Frehel, C., P. Robbe, R. Tinelli, and A. Ryter. 1982. Relationship between biochemical and cytochemical results obtained on *Bacillus megaterium* and *Bacillus subtilis* cell-wall polysaccharides. *J. Ultrastruct. Res.* **81**:78-87.
11. Gerhardt, P., and R. Scherrer. 1974. Porosities of microbial cell walls and protoplast membranes. *Proc. Int. Congr. Int. Assoc. Microbiol. Soc.* **1**:506-513.
12. Graham, L. L. 1992. Freeze-substitution studies of bacteria. *Electron Microsc. Rev.* **5**:77-103.
13. Graham, L. L., and T. J. Beveridge. 1990. Evaluation of freeze-substitution and conventional embedding protocols for routine electron microscopic processing of eubacteria. *J. Bacteriol.* **172**:2141-2149.
14. Graham, L. L., and T. J. Beveridge. 1990. Effect of chemical fixatives on accurate preservation of *Escherichia coli* and *Bacillus subtilis* structure in cells prepared by freeze-substitution. *J. Bacteriol.* **172**:2150-2159.
- 14a. Graham, L. L., and T. J. Beveridge. 1990. Structural differentiation of the *Bacillus subtilis* 168 cell wall, abstr. J1, p. 217. Abstr. 90th Annu. Meet. Am. Soc. Microbiol. 1990. American Society for Microbiology, Washington, D.C.
15. Graham, L. L., R. Harris, W. Villiger, and T. J. Beveridge. 1991. Freeze-substitution of gram-negative eubacteria: general cell morphology and envelope profiles. *J. Bacteriol.* **173**:1623-1633.
16. Hobot, J. A., and H. J. Rogers. 1991. Intracellular localization of the autolytic *N*-acetylmuramyl-L-alanine amidase in *Bacillus subtilis* 168 and in an autolysis-deficient mutant by immunoelectron microscopy. *J. Bacteriol.* **173**:961-967.
17. Hughes, R. C., and P. J. Tanner. 1968. The action of dilute alkali on some bacterial cell walls. *Biochem. Biophys. Res. Commun.* **33**:22-28.
18. Koch, A. L. 1983. The surface stress theory of microbial morphogenesis. *Adv. Microb. Physiol.* **24**:301-366.
19. Lang, W. K., and A. R. Archibald. 1983. Relation between wall teichoic acid content and concanavalin A binding in *Bacillus subtilis* 168. *FEMS Microbiol. Lett.* **20**:163-166.
20. Mauck, J., L. Chan, L. Glaser, and J. Williamson. 1972. Mode of cell wall growth of *Bacillus megaterium*. *J. Bacteriol.* **109**:373-378.
21. Merad, T., A. R. Archibald, I. C. Hancock, C. R. Harwood, and J. A. Hobot. 1989. Cell wall assembly in *Bacillus subtilis*: visualization of old and new wall material by electron microscopic examination of samples stained selectively for teichoic acid and teichu-

- ronic acid. J. Gen. Microbiol. **135**:645-655.
22. Mobley, H. L. T., A. L. Koch, R. J. Doyle, and U. N. Streips. 1984. Insertion and fate of the cell wall in *Bacillus subtilis*. J. Bacteriol. **158**:169-179.
 23. Osborn, M. J., K. E. Gander, and E. Parisi. 1972. Mechanism of assembly of outer membrane of *Salmonella typhimurium*: isolation and characterization of cytoplasmic and outer membrane. J. Biol. Chem. **247**:3973-3986.
 24. Pooley, H. M. 1976. Turnover and spreading of old wall during surface growth of *Bacillus subtilis*. J. Bacteriol. **125**:1127-1138.
 25. Pooley, H. M. 1976. Layered distribution, according to age, within the cell wall of *Bacillus subtilis*. J. Bacteriol. **125**:1139-1147.
 26. Reynolds, E. S. 1963. Use of lead citrate as a stain in electron microscopy. Cell Biol. **17**:208-213.
 27. Scherrer, R., and P. Gerhardt. 1971. Molecular sieving by the *Bacillus megaterium* cell wall and protoplast. J. Bacteriol. **107**:718-735.
 28. Sonnenfeld, E. M., T. J. Beveridge, and R. J. Doyle. 1985. Discontinuity of charge on cell wall poles of *Bacillus subtilis*. Can. J. Microbiol. **31**:875-877.
 29. Sonnenfeld, E. M., T. J. Beveridge, A. L. Koch, and R. J. Doyle. 1985. Asymmetric distribution of charge on the cell wall of *Bacillus subtilis*. J. Bacteriol. **163**:1167-1171.
 30. Spizizen, J. 1958. Transformation of biochemically deficient strains of *Bacillus subtilis* by deoxyribonucleate. Proc. Natl. Acad. Sci. USA **44**:1072-1078.
 31. Tempest, D. W. 1969. Quantitative relationships between inorganic cations and anionic polymers in growing bacteria. Proc. Gen. Soc. Microbiol. **19**:87-111.
 32. Tsien, H. C., G. D. Shockman, and M. L. Higgins. 1978. Structural arrangement of polymers within the wall of *Streptococcus faecalis*. J. Bacteriol. **133**:372-386.
 33. Zar, J. H. 1984. Biostatistical analysis, 2nd ed. Prentice-Hall, Inc., Englewood Cliffs, N.J.